



Stress hysteresis and temperature dependence of phase transition stress in nanostructured NiTi—Effects of grain size

Aslan Ahadi and Qingping Sun

Citation: [Applied Physics Letters](#) **103**, 021902 (2013); doi: 10.1063/1.4812643

View online: <http://dx.doi.org/10.1063/1.4812643>

View Table of Contents: <http://scitation.aip.org/content/aip/journal/apl/103/2?ver=pdfcov>

Published by the [AIP Publishing](#)

Articles you may be interested in

[Superelastic memory effect in in-situ NbTi-nanowire-NiTi nanocomposite](#)

Appl. Phys. Lett. **101**, 173115 (2012); 10.1063/1.4764538

[Effects of phase transition on the hardness of shape memory alloys](#)

Appl. Phys. Lett. **94**, 261906 (2009); 10.1063/1.3160740

[Temperature-dependent quantitative \$3\omega\$ scanning thermal microscopy: Local thermal conductivity changes in NiTi microstructures induced by martensite-austenite phase transition](#)

Rev. Sci. Instrum. **79**, 093703 (2008); 10.1063/1.2982235

[The nano- and mesoscopic cooperative collective mechanisms of inhomogeneous elastic-plastic transitions in polycrystalline TiNi shape memory alloys](#)

J. Appl. Phys. **101**, 103522 (2007); 10.1063/1.2722239

[A Low Hysteresis NiTiFe Shape Memory Alloy Based Thermal Conduction Switch](#)

AIP Conf. Proc. **824**, 3 (2006); 10.1063/1.2192327

The image shows the cover of the journal Applied Physics Reviews. It features a blue and orange color scheme with a molecular structure in the background. The text 'AIP Applied Physics Reviews' is at the top left. The main title 'NEW Special Topic Sections' is in large white letters. Below it, 'NOW ONLINE' is in orange, followed by 'Lithium Niobate Properties and Applications: Reviews of Emerging Trends' in white. The AIP logo and 'Applied Physics Reviews' are at the bottom right.

NEW Special Topic Sections

NOW ONLINE
Lithium Niobate Properties and Applications:
Reviews of Emerging Trends

AIP Applied Physics
Reviews

Stress hysteresis and temperature dependence of phase transition stress in nanostructured NiTi—Effects of grain size

Aslan Ahadi and Qingping Sun^{a)}

Department of Mechanical Engineering, The Hong Kong University of Science and Technology, Hong Kong, China

(Received 15 May 2013; accepted 11 June 2013; published online 9 July 2013)

Stress hysteresis (H) and temperature dependence of phase transition stress ($d\sigma/dT$) are the two signatures of first-order phase transition in shape memory alloys. We studied the effects of grain size on these two properties in polycrystalline superelastic NiTi with the average grain size from 10 nm to 1500 nm. We identified a critical grain size (~ 60 nm) below which both H and $d\sigma/dT$ rapidly decrease, leading to vanishing hysteresis and breakdown of Clausius-Clapeyron equation. The physics behind such grain size effects are the dominance of interfacial energy in the energetics of the polycrystal and the lack of two-phase coexistence at nano-scales. © 2013 AIP Publishing LLC. [<http://dx.doi.org/10.1063/1.4812643>]

Stress-strain ($\sigma - \varepsilon$) hysteresis loop (H) and temperature dependence of transition stress ($d\sigma/dT$) are the two signatures of the thermoelastic first-order martensitic phase transition (PT) in shape memory alloys (SMAs) and are widely observed in polycrystalline SMA systems such as NiTi and CuAlNi.^{1,2} With the fast development of nanostructured materials and the race for better materials performance, extreme grain refinement and nano-scale PT have become active topics of research in recent years since grain size (GS) is a key microstructural factor in controlling physical and mechanical behavior of polycrystals.^{3–6} It has been reported that the H of the nanostructured polycrystalline NiTi SMA is very sensitive to the GS^{7,8} and that the thermally-induced martensitic PT can be completely suppressed when the GS falls below 60 nm.⁹ In many applications, H and $d\sigma/dT$ are the most important properties^{10,11} and design parameters of the SMA device and structures. In the nano-scale GS regime, systematic experiments to examine the effects of GS on the PT behavior and these two properties are important and have not been available so far.

In this letter, we first fabricate polycrystalline superelastic NiTi with average GS from 10 nm to 1500 nm using severe cold working and heat treatment and then investigate the effects of GS on H and $d\sigma/dT$ of the material. We analyze the experimental results, explore the physical origins, and give thermodynamics explanations for the observed phenomena.

Superelastic NiTi sheet with chemical composition of Ti-50.9 at. %Ni was cold-rolled to 42% thickness reduction and heat treated according to two batches of heat treatments. For batch 1 (recovery and recrystallization annealing), the specimens were annealed at temperatures of 250, 300, 350, 400, 450, 500, 550, and 600 °C for 45 min followed by water quenching. For batch 2 (recrystallization annealing), the specimens were annealed well above the recrystallization temperature (~ 350 °C) at 485 °C for 2 min and 520 °C for 2, 3, and 6 min followed by water quenching (see Table I). Average GS of the each heat treated specimen was measured using *in situ* high temperature XRD

(Williamson-Hall method)¹² and was double-checked by dark-field TEM (DFTEM) technique in a JEOL 2010F high resolution TEM. Dog-bone tensile specimens (1 mm thickness, 1.3 mm width, and 17.3 mm gauge length) were cut along the rolling direction and were used for mechanical tests. To measure H and $d\sigma/dT$, isothermal tensile tests at different constant temperatures were performed in a Universal Testing Machine (UTM). Latent heat release during PT was characterized by *in situ* measurement of specimen's temperature oscillation in displacement-controlled cyclic loading/unloading tensile tests on an MTS 858 universal machine at frequency of 0.05 Hz. An ultra-thin K-type thermocouple with diameter of 0.025 mm (response time of 0.05 s) was taped to the specimen surface to capture the temperature evolution.¹³ Prior to the tests, the samples were trained at a low frequency (isothermal condition) to remove the cyclic plasticity.¹⁴

Fig. 1(a) shows a set of representative bright-field TEM microstructures obtained after cold rolling and heat treatment according to batch 1 and batch 2. Annealing at temperature of 300 °C promotes partial devitrification and recovery of the deformed lattice and results in average GS of 27 nm. Annealing at 520 °C for 3 and 6 min produces a fully recrystallized microstructure with average GS of 64 and 80 nm, respectively. Fig. 1(b) is a summary of GS measurements by *in situ* XRD (black squares) and DFTEM (red circles). It is seen that GS monotonically increases from 10 nm for the cold-rolled NiTi to 1500 nm for NiTi annealed at 600 °C.

Fig. 2(a) displays the isothermal tensile stress-strain curves for specimens of different GS. The steady-state temperature evolutions in cyclic loading/unloading are shown in Fig. 2(b). It is seen that stress-induced PT can occur for specimens of all GS as evidenced by the hysteresis loop of a reversible deformation cycle and the release/absorption of latent heat from the PT. With the decrease of GS, the phase transition stress increased and hysteresis loop area decreased monotonically. According to the recent study,^{13,15} the amplitude of temperature oscillation (ΔT) in a cyclic PT simply scales with the amount of the specific latent heat (l_0) of the polycrystal according to

^{a)} Author to whom correspondence should be addressed. Electronic mail: meqpsun@ust.hk. Tel.: (852) 23588655. Fax: (852) 23581543

TABLE I. Average grain size and thermomechanical properties of the nanostructured NiTi.

Material	Thermomechanical properties					
	Average grain size (nm)	Transformation strain, ϵ_{tr}	Temp. oscillation amplitude ΔT ($^{\circ}\text{C}$)	l_0 (J/g)	$d\sigma/dT$ (Experiment) MPa/K	$d\sigma/dT$ (Eq. (5)) MPa/K
Cold-rolled	10	N/A	7.42	3.8	0.3	N/A
Batch 1 (250 $^{\circ}\text{C}$ -45 min)	18	N/A	N/A	N/A	3.54	N/A
Batch 1 (300 $^{\circ}\text{C}$ -45 min)	27	N/A	10.04	6.5	4.8	N/A
Batch 2 (485 $^{\circ}\text{C}$ -2 min)	32	N/A	14.43	7.44	5.22	N/A
Batch 2 (520 $^{\circ}\text{C}$ -2 min)	42	N/A	15.88	8.1	5.8	N/A
Batch 2 (520 $^{\circ}\text{C}$ -3 min)	64	0.031	18	9.3	6	6.65
Batch 2 (520 $^{\circ}\text{C}$ -6 min)	80	0.04	20.18	10.41	6.25	6.08
Batch 1 (600 $^{\circ}\text{C}$ -45 min)	1500	0.042	≈ 21	≈ 12	6.5	≈ 5.9

$$\Delta T = \frac{l_0}{\lambda \sqrt{1 + \frac{1}{f^2 4\pi^2 t_h^2}}}, \quad (1)$$

where λ is the heat capacity per unit volume, f is the loading frequency, and t_h is characteristic lumped heat convection time of the specimen in a given ambient.¹³ From Fig. 2(b), it is seen that the finer the GS, the smaller the amplitude of temperature oscillation and therefore the smaller value of l_0 (see Table I). There are two reasons leading to the decrease of l_0 with GS. The first reason is the increase of the grain boundary volume fraction with the decrease of GS.¹⁶ Assuming grain boundary thickness as 1 nm, grain boundary

zones occupy approximately 27% of the volume for GS = 10 nm. The second reason is that for smaller GS, a larger stress is required for the PT (see inset of Fig. 2(a)). For a given total strain of 4%, this means a larger portion of elastic strain, a smaller portion of transformation, and therefore a smaller l_0 since the released latent heat scales with the amount of transformation.¹⁷ This is, in fact, due to a gradual suppression of stress-induced PT with GS reduction below 60 nm which at the same time promotes elastic strain. Here, we see that although thermally-induced martensitic PT is totally suppressed for GS below 60 nm,⁹ PT can still be induced by stress for GS as small as 10 nm as evidenced by the measured l_0 and the small hysteresis loop area.

The variation of isothermal hysteresis loop area (H) with GS is shown in Fig. 3(a) for loading-unloading cycles with a maximum strain of 5%. It is seen that when GS is larger than 80 nm there is a little change in H and that when

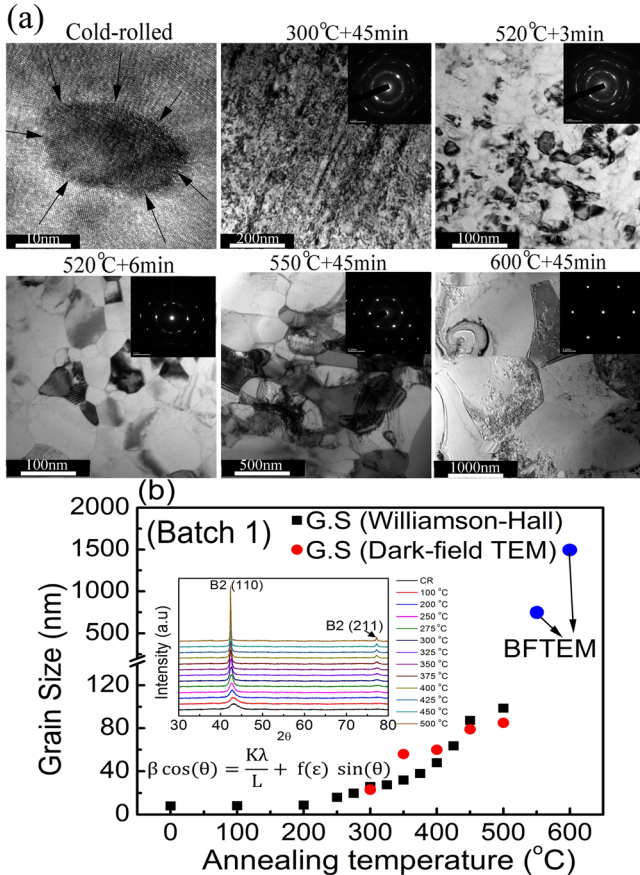


FIG. 1. (a) TEM images of the microstructure before and after the heat treatments. Black arrows point to a grain survived from amorphisation after cold-rolling. (b) Range of GS achieved in the heat treatments (color online).

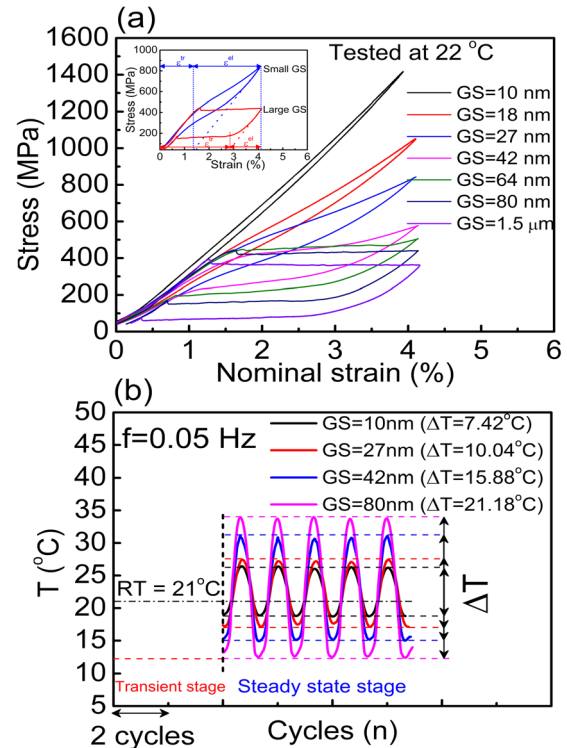


FIG. 2. GS effects on (a) stress-strain curves, and (b) steady-state temperature evolution (heating and cooling) in cyclic loading/unloading, showing the release/absorption of latent heat from the stress-induced PT (color online).

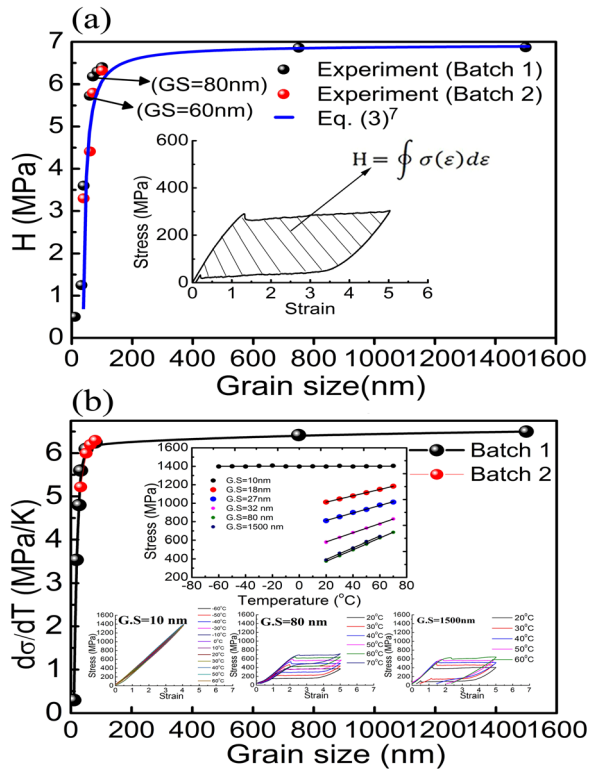


FIG. 3. (a) Variation of the measured H with GS and the comparison with the simple model prediction from Eq. (3). (b) Variation of $d\sigma/dT$ with GS, showing a very weak sensitivity of the phase transition stress to the temperature at nano-length scales ($GS < 60$ nm) (color online).

$GS < 60$ nm H decreases rapidly. The value of H for $GS = 32$ nm ($H = 1.25$ MPa) is about 5.5 times smaller than that for the largest GS ($H = 6.87$ MPa). The measured $d\sigma/dT$ for specimens of different GS is shown in Fig. 3(b) where, as an indicative measure, the value of stresses at the fixed strain of 4% in loading and different constant temperatures are used to calculate $d\sigma/dT$. It is seen that different from traditional polycrystalline NiTi where $d\sigma/dT$ is about 7 MPa/K,^{18,19} $d\sigma/dT$ decreased rapidly when the GS falls below 60 nm. For $GS = 10$ nm, the PT becomes almost insensitive to the temperature and the superelasticity can be preserved in a much larger temperature window from 60 to -60 °C (see inset of Fig. 3(b)).

The above results show that NiTi polycrystals with extremely small GS behave very differently from the traditional coarse-grained counterparts with $GS > 100$ nm. Both H and $d\sigma/dT$ of the polycrystal, which are the two important signatures of the first-order PT, decrease with the GS and tend to vanish when the GS is reduced to the nano length-scale. To understand the strong GS dependence of H and $d\sigma/dT$, one must, among the other possible factors, consider the effects of the internal length-scales (i.e., GS and austenite/martensite interface thickness) of the polycrystalline material on the energetics and dynamics of the PT. Especially, we should notice the difference between the classical thermodynamics relationships established for homogenous systems (phases) and the macroscopic response of polycrystal which is in fact an aggregate consisting of large numbers of nanograins and phase interfaces. In the following, we will take into account the length scales of such material's multi-scaled structural hierarchy and try to provide explanations for the above GS effects.

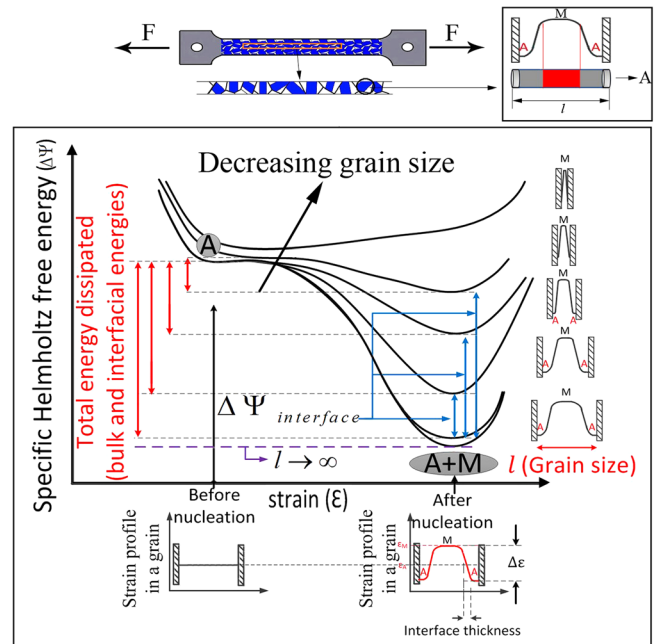


FIG. 4. Schematic representation of GS effect on the amount of energy dissipation during stress-induced PT inside a grain in loading process (color online).

From thermodynamics point of view, the macroscopic isothermal stress hysteresis of a polycrystalline material means mechanical energy dissipation in a phase transition cycle. One commonly accepted view of the hysteresis is that it is the consequence of the internal heterogeneity of the polycrystalline system, the free energy of which has multiple metastable minima.^{20,21} As the PT proceeds, the material experiences many micro-scale instabilities via nucleation and growth of martensite domains. When the state of the system moves from one metastable local minimum to the other, energy is dissipated and the amount is equal to the free energy change (see the schematic illustration in Fig. 4).²² For the stress-induced PT process in polycrystalline NiTi, it has been shown that^{7,23} the hysteresis originates from the nucleation of martensite in individual grains as the result of numerous microscopic instability of the system. To illustrate the GS effect on hysteresis (dissipation) in the simplest way, we consider the specific Helmholtz free energy change $\Delta\Psi$ of a single one-dimensional cylindrical grain before and after PT under external stretching as shown in Fig. 4. $\Delta\Psi$ consists of bulk ($\Delta\Psi_{bulk}$, negative) and interfacial ($\Delta\Psi_{interface}$, positive) contributions

$$\begin{aligned}\Delta\Psi &= \Delta\Psi_{bulk} + \Delta\Psi_{interface} = \Delta\Psi_{bulk} + \frac{A}{V}\gamma_{interface} \\ &= \Delta\Psi_{bulk} + \frac{A}{A \cdot l}\gamma_{interface},\end{aligned}\quad (2)$$

where V , A , and l are, respectively, the volume, cross-section area, and length (GS) of the 1D $\gamma_{interface}$ is the specific interfacial energy and scales with austenite/martensite interface thickness (l_m).^{7,24,25} From Eq. (2), the variations of $\Delta\Psi$ with GS are schematically shown in Fig. 4. The two energy wells represent the energies of equilibrium states before and after PT, and the difference represents the total amount of energy dissipated during the forward PT. It is seen that $\Delta\Psi_{interface}$ increases with

decrease of l (blue arrows), which makes $\Delta\Psi$ to decrease (red arrows) and therefore dissipation (hysteresis) becomes smaller. In fact, when l is reduced below a critical size, the specific interfacial energy term overwhelmingly dominates the total energetics of the system. As such, the system becomes more stable and hysteresis tends to vanish.^{7,26} Based on the above rationale, a multiscale model is established recently,⁷ where the variation of hysteresis loop area (H) with GS(l) can be approximated by a simple scaling law as

$$H = H_0 \left(1 - \frac{l_m}{l} \right), \quad (3)$$

where H_0 is the hysteresis loop area of the coarse-grained polycrystal and l_m is austenite/martensite interface thickness. From Eq. (3), it is seen that reducing GS to the interface thickness which is the order of a few nanometers can indeed lead to the vanishing of hysteresis of polycrystalline NiTi. From the comparison between Eq. (3) and experimental data in Fig. 3, it is seen that Eq. (3) can well capture the observed GS dependence of hysteresis.

In order to explain the observed rapid decrease of $d\sigma/dT$ with GS, one has to reexamine the conditions for the classical Clausius-Clapeyron equation for liquid-gas first-order PT²⁷

$$\frac{dP}{dT} = \frac{\Delta S}{\Delta V} = \frac{l_0}{T\Delta V}, \quad (4)$$

where P is the equilibrium pressure for the two-phase coexistence, ΔS and ΔV are the jumps in entropy and volume, l_0 is the specific latent heat, and T is the equilibrium temperature of the two phases in the phase diagram. For PT in SMA bulk single crystal and coarse-grained polycrystals under tensile stress (σ), we have the well-established temperature dependence of phase transition stress^{28,29}

$$\frac{d\sigma}{dT} = \frac{\Delta S}{\Delta \varepsilon} = \frac{l_0}{T\varepsilon_{tr}}, \quad (5)$$

where $\Delta \varepsilon = (\varepsilon_{tr})$ is the jump in strain across the austenite/martensite interface or is called transformation strain (ε_{tr}). It should be noticed that Eqs. (4) and (5) are derived based on the condition of two-phase coexistence (each phase has distinct state variables) at the equilibrium pressure (stress) in the $P - T$ or $\sigma - T$ phase diagram (see Fig. 5(a)). The experimental results of $d\sigma/dT$ and some results from Eq. (5) are listed in Table I. It is seen that for the NiTi with GS = 64, 80, and 1500 nm the predicted values of $d\sigma/dT$ from Eq. (5) are close to the experimental measurements, indicating the validity of the equation for the polycrystalline NiTi in this range of GS. However, when the GS is below 64 nm, the experimental data of ε_{tr} are no longer available since the structure changes in such small grains are much less distinct (i.e., the jumps in the order parameter (strain) and the entropy become less clear, see Fig. 5(b)). We have to consider the effects of the additional degrees of freedom such as grain size (l) and austenite/martensite interface thickness (l_m) on the energetics of the PT. The key factor is that due to the constraint of grain boundaries in nanograins, the PT events occur within an extremely small space where interface thickness and GS become comparable. The transition from one phase to another cannot happen via

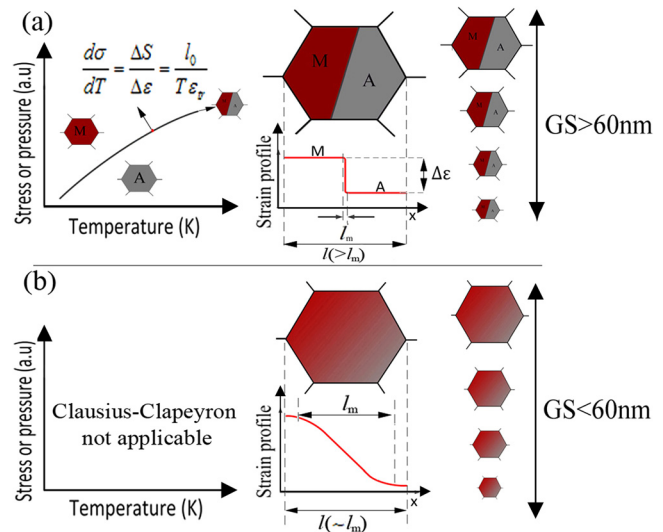


FIG. 5. Stress (or pressure)-temperature phase diagram for (a) coarse-grained and (b) nano-grained NiTi (color online).

nucleation and growth as in the coarse-grained polycrystals since there is no space in each grain to accommodate the two-phase coexistence (as in Fig. 5(b)). The PT tends to become a continuous, stable, and therefore reversible process. The overall response of the polycrystal approaches the reversible elasticity and thus gradually loses its temperature dependence. This scenario is supported by our recent *in situ* X-ray diffraction (XRD) experiments (not shown here due to the limit of the space) where a continuous reversible shift in peak position of the remnant austenite phase during loading/unloading up to strain of 5% was observed for specimens with GS < 60 nm indicating the continuous elastic deformation of the austenite phase. That means, below GS = 60 nm, there is a change in the pseudoelastic deformation mechanism by phase transformation strain (with two-phase coexistence, hysteresis loop, and latent heat release) to the reversible elastic structural change (with small hysteresis loop, small latent heat release, and weak temperature dependence). In the limiting case, both $l_0 (= T \cdot \Delta S)$ and $\Delta \varepsilon$ approaches zero, and $d\sigma/dT$ will have 0/0 type indeterminacy like those in second order PT.^{27,30} In such nano-scale, the classical Clausius-Clapeyron equation derived for the first-order PT loses its physical meaning and breaks down in predicting the observed decrease in $d\sigma/dT$ (see Fig. 5(b)).

It should be noticed that some partial amorphous phase and highly strained nano grains survived in the specimens (heat treated in the recovery regime (<300 °C)) might also affect H and $d\sigma/dT$.³¹ However, the fact that the same trend is observed from both batches of heat treatment indicates that these factors may have minor contribution to the observed GS effect.

In summary, we have observed systematic changes in the hysteresis loop area (H) and temperature dependence of phase transition stress ($d\sigma/dT$) with the GS. When the GS falls below a critical value (~ 60 nm), both H and $d\sigma/dT$ decreases rapidly and tend to vanish. The macroscopic response of the nanostructured polycrystal exhibits unusual characteristics such as extremely small mechanical energy dissipation, small amount of latent heat, and very weak temperature dependence of phase transition stress as compared with the coarse-grained counterparts. Such significant GS effect on the PT behavior of the material is primarily caused

by the gradual dominance of interfacial energy in the energetics of the polycrystalline system, leading to the reversible elastic response and the breakdown of Clausius-Clapeyron equation. The results obtained encourage the development of nanostructured NiTi polycrystalline SMAs with extremely small H and $d\sigma/dT$, but still preserving large reversible deformation, which may open up some important possibilities such as high fatigue-resistance and low rate dependence in the application of this kind of smart material.

The authors are grateful to the RGC of Hong Kong for the financial support to the research of this paper through the GRF grant (project No. GRF619511).

¹K. Otsuka and C. M. Wayman, *Acta Metall.* **24**, 207 (1976).

²S. Miyazaki, K. Otsuka, and Y. Suzuki, *Scr. Metall.* **15**, 287 (1981).

³T. Waitz, D. Spišák, J. Hafner, and H. P. Karnthaler, *Europhys. Lett.* **71**, 98 (2005).

⁴J. Ye, R. K. Mishra, A. R. Pelton, and A. M. Minor, *Acta Mater.* **58**, 490 (2010).

⁵T. Waitz, *Acta Mater.* **53**, 2273 (2005).

⁶Y. Estrin and A. Vinogradov, *Acta Mater.* **61**, 782 (2013).

⁷Q. P. Sun and Y. J. He, *Int. J. Solids Struct.* **45**, 3868 (2008).

⁸Y. Kim, G. Cho, S. Hur, S. Jeong, and T. Nam, *Mater. Sci. Eng., A* **438–440**, 531 (2006).

⁹T. Waitz, V. Kazykhanov, and H. P. Karnthaler, *Acta Mater.* **52**, 137 (2004).

¹⁰J. Cui, Y. S. Chu, O. O. Famodu, Y. Furuya, J. Hattrick-Simpers, R. D. James, A. Ludwig, S. Thienhaus, M. Wuttig, Z. Zhang, and I. Takeuchi, *Nature Mater.* **5**, 286 (2006).

¹¹Z. Zhang, R. D. James, and S. Müller, *Acta Mater.* **57**, 4332 (2009).

¹²C. E. Krill and R. Birringer, *Philos. Mag.* **77**, 621 (1998).

¹³H. Yin and Q. P. Sun, *J. Mater. Eng. Perform.* **21**, 2505 (2012).

¹⁴S. Miyazaki, T. Imai, Y. Igo, and K. Otsuka, *Metall. Mater. Trans. A* **17**, 115 (1986).

¹⁵Y. J. He and Q. P. Sun, *Smart Mater. Struct.* **19**, 1 (2010).

¹⁶P. Barai and G. J. Weng, *Int. J. Plast.* **25**, 2410 (2009).

¹⁷F. Falk, *Acta Metall.* **28**, 1773 (1980).

¹⁸J. A. Shaw and S. Kyriakides, *Acta Mater.* **45**, 683 (1997).

¹⁹Y. Liu and H. Yang, *Smart Mater. Struct.* **16**, S22 (2007).

²⁰J. Ortin and L. Delaey, *Int. J. Non-Linear Mech.* **37**, 1275 (2002).

²¹G. Bertotti, *Phys. Rev. Lett.* **76**, 1739 (1996).

²²G. Puglisi and L. Truskinovsky, *J. Mech. Phys. Solids* **53**, 655 (2005).

²³R. Abeyaratne, C. Chu, and R. D. James, *Philos. Mag. A* **73**, 457 (1996).

²⁴P. M. Chaikin and T. C. Lubensky, *Principles of Condensed Matter Physics* (Cambridge University Press, New York, 1995), p. 597.

²⁵F. Falk, *J. Solid State Phys.* **20**, 2501 (1987).

²⁶A. Vainchtein and P. Rosakis, *J. Nonlinear Sci.* **9**, 697 (1999).

²⁷C. N. R. Rao and K. J. Rao, *Phase Transitions in Solids*, 1st ed. (McGraw-Hill, 1977).

²⁸K. Otsuka and C. M. Wayman, *in Shape Memory Materials*, 1st ed., edited by J. Van Humbeeck and R. Stalmans (Cambridge University Press, Cambridge, 1998).

²⁹P. Wollants, M. De Bonte, and J. R. Roos, *Z. Metallkd.* **70**, 113 (1979).

³⁰C. N. R. Rao, *Bull. Mater. Sci.* **3**, 75 (1981).

³¹K. Tsuchiya, Y. Hada, T. Koyano, K. Nakajima, M. Ohnuma, T. Koike, Y. Todaka, and M. Umemoto, *Scr. Mater.* **60**, 749 (2009).